Letters

Open-Phase Fault Detection in Delta-Connected PMSM Drive Systems

Jun Hang, *Member, IEEE*, Shichuan Ding, *Member, IEEE*, Jianzhong Zhang, *Senior Member, IEEE*,
Ming Cheng, *Fellow, IEEE*, and Qunjing Wang

***Abstract*—This letter presents an open-phase fault detection method for delta-connected permanent magnet synchronous machine (PMSM) drive systems. This method is based on zero sequence current component (ZSCC) and stator currents. First, the model of the delta-connected PMSM is established under healthy and fault conditions. Then, the expression of the ZSCC is presented, and fault indicators are defined based on the ZSCC and stator currents, which are used for the open-phase fault detection and location. Finally, both the simulation and experimental results validate the effectiveness of the proposed method.**

***Index Terms*—Fault detection and location, open-phase fault, permanent magnet synchronous machine (PMSM).**

I. INTRODUCTION

NOWADAYS, permanent magnet synchronous machines (PMSM) are widely used in electrical vehicles, wind energy systems, and subways due to their inherent advantages of high power density and high efficiency. In these occasions, the reliability of the PMSM is greatly important. An open-phase fault is the common fault for the PMSM drive system [1]. The fault can cause large electromagnetic torque ripples and serious mechanical vibration. If this fault is not detected in time, and the remedial measures or fault-tolerant schemes are not taken, the successive operation of the PMSM may cause the secondary damage, even catastrophic failure to the overall system.

As known, the fault detection is the precondition of the fault tolerance. However, most of the previous studies about the open-phase fault focused on the fault tolerance in recent years [2]–[12], while the relatively few studies focused on the open-phase fault detection. In [12], the open-phase fault is detected by the root-mean-square value of phase currents. In [13], the open-phase fault is detected by frequency-domain analysis and $\alpha\beta$ current signature. In [14], the single open-phase fault detection is achieved by the predictive method, which is based on the difference between actual stator current and its predicted value. In [15], an open-phase fault detection method is presented based on *d*-axis and *q*-axis (DQ) current signature. In [16], a method is presented for the open-phase fault detection and discrimination for the PMSM drive system, where the discrimination of the fault types is achieved. In [17], the symmetrical components theory is developed for the open-phase fault detection of the five-phase PMSM drive system. The methods proposed in [12]–[17] focused on the wye-connected PMSM drive system, and they may be not suitable for the delta-connected PMSM drive system. As known, the wye-connected and delta-connected windings are both common in the ac machine. Hence, it is also necessary for fault detection toward the delta-connected PMSM. However, the delta-connected PMSM with the open-phase fault is rarely studied so far.

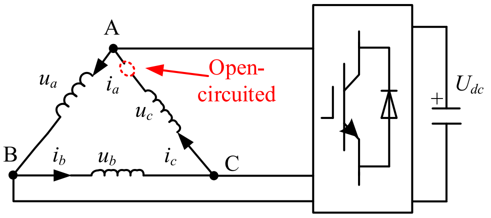

Fig. 1. Delta-connected PMSM with the inverter.

This letter proposes an open-phase fault detection method for the delta-connected PMSM drive system, which is based on zero sequence current component (ZSCC) and stator currents. The fault indicators are defined based on the ZSCC and stator currents, which are used for the open-phase fault detection and location. Finally, the simulation and experimental platforms are established to validate the proposed method.

II. DELTA-CONNECTED PMSM

Fig. 1 shows three-phase delta-connected PMSM with the inverter. The voltage equations of three-phase healthy delta-connected PMSM in *abc* reference frame is expressed as

Manuscript received June 7, 2017; revised September 25, 2017; accepted November 6, 2017. Date of publication November 12, 2017; date of current version April 20, 2018. This work was supported in part by the National Natural Science Foundation of China under Grant 51637001, Grant 51607001, and Grant 51507002 and in part by the Natural Science Foundation of Anhui Province (1708085QE108, 1508085ME87). *(Corresponding author: Jun Hang.)*

J. Hang and S. Ding are with the National Engineering Laboratory of Energy-Saving Motor & Control Technique and the School of Electrical Engineering and Automation, Anhui University, Hefei 230601, China (e-mail: jun_hang511@163.com; dingsc@126.com).

J. Zhang and M. Cheng are with the School of Electrical Engineering, Southeast University, Nanjing 210096, China (e-mail: jiz@seu.edu.cn; mcheng@seu.edu.cn).

Q. Wang is with the Collaborative Innovation Center of Industrial Energy-Saving and Power Quality Control and the Engineering Research Center of Power Quality, Ministry of Education, Anhui University, Hefei 230601, China (e-mail: wangqunjing@ahu.edu.cn).

Color versions of one or more of the figures in this letter are available online at http://ieeexplore.ieee.org.

Digital Object Identifier 10.1109/TPEL.2017.2772793

[16]

$$\begin{cases} u_a = R_s i_a + L\dfrac{di_a}{dt} + M\dfrac{di_b}{dt} + M\dfrac{di_c}{dt} + \dfrac{d\lambda_{PM,a}}{dt} \\ u_b = R_s i_b + M\dfrac{di_a}{dt} + L\dfrac{di_b}{dt} + M\dfrac{di_c}{dt} + \dfrac{d\lambda_{PM,b}}{dt} \\ u_c = R_s i_c + M\dfrac{di_a}{dt} + M\dfrac{di_b}{dt} + L\dfrac{di_c}{dt} + \dfrac{d\lambda_{PM,c}}{dt} \end{cases} \tag{1}$$

where u_a, u_b, and u_c are the phase voltages, i_a, i_b, and i_c are the phase currents, R_s is the phase stator resistance, L is the phase stator self-inductance, and M is the mutual inductance between the stator phases. $\lambda_{PM,a}$, $\lambda_{PM,b}$, and $\lambda_{PM,c}$ are the flux in the phases a, b, and c due to permanent magnets, respectively, and they are expressed as [16]

$$\begin{cases} \lambda_{PM,a} = \lambda_{PM,1}\cos(\theta) + \sum_{v=2k+1}\lambda_{PM,v}\cos(v\theta - \theta_v) \\ \lambda_{PM,b} = \lambda_{PM,1}\cos\left(\theta - \dfrac{2\pi}{3}\right) + \sum_{v=2k+1}\lambda_{PM,v} \\ \qquad \times \cos\left(v\theta - \theta_v - 2v\dfrac{\pi}{3}\right) \\ \lambda_{PM,c} = \lambda_{PM,1}\cos\left(\theta + \dfrac{2\pi}{3}\right) + \sum_{v=2k+1}\lambda_{PM,v} \\ \qquad \times \cos\left(v\theta - \theta_v + 2v\dfrac{\pi}{3}\right) \end{cases} \tag{2}$$

where k is a positive integer, $\lambda_{PM,1}$ is the amplitude of the fundamental magnet flux, $\lambda_{PM,v}$ is the amplitude of the v_{th} harmonic magnet flux, θ is the rotor electrical position, and θ_v is the angle between the v_{th} harmonic magnet flux and the fundamental one.

Supposing the stator winding of the phase c is open circuited, as shown in Fig. 1, the voltage equation of the stator phase c does not exist, and the stator current i_c is equal to zero. Hence, under the fault condition, the voltage equations of the delta-connected PMSM are expressed as

$$\begin{cases} u_a = R_s i_a + L\dfrac{di_a}{dt} + M\dfrac{di_b}{dt} + \dfrac{d\lambda_{PM,a}}{dt} \\ u_b = R_s i_b + M\dfrac{di_a}{dt} + L\dfrac{di_b}{dt} + \dfrac{d\lambda_{PM,b}}{dt} \end{cases} \tag{3}$$

III. FAULT DETECTION

A. Healthy Condition

According to Kirchhoff's voltage law, the sum of three-phase voltages of a delta-connected PMSM is equal to zero, and expressed as

$$u_a + u_b + u_c = 0. \tag{4}$$

By substituting (1) into (4), it results in

$$R_s(i_a + i_b + i_c) + (L + 2M)\frac{d(i_a + i_b + i_c)}{dt} + \frac{d}{dt}(\lambda_{PM,a} + \lambda_{PM,b} + \lambda_{PM,c}) = 0. \tag{5}$$

The ZSCC is defined as

$$i_{zsc} = i_a + i_b + i_c. \tag{6}$$

By substituting (2) and (6) into (5), it yields

$$R_s i_{zsc} + (L + 2M)\frac{di_{zsc}}{dt} = -\frac{d\lambda_{PM,0}}{dt} \tag{7}$$

where

$$\begin{aligned} \lambda_{PM,0} &= \lambda_{PM,a} + \lambda_{PM,b} + \lambda_{PM,c} \\ &= 3\sum_{v=3n,n=1,3,5\ldots}\lambda_{PM,v}\cos(v\theta - \theta_v). \end{aligned} \tag{8}$$

Based on (7) and (8), it is known that i_{zsc} depends only on the time derivative of $\lambda_{PM,0}$. Hence, i_{zsc} is constituted only by the $3n(n = 1, 3, 5, \ldots)$ order harmonic components.

B. Open-Phase Fault Condition

In the case that the fault occurs in the phase c, the stator current i_c is equal to zero. Hence, i_{zsc} is expressed as

$$i_{zsc} = i_a + i_b. \tag{9}$$

By submitting (9) into (4), it has

$$\begin{aligned} R_s i_{zsc} + (L + M)\frac{di_{zsc}}{dt} &= (u_a + u_b) \\ &- \left(\frac{d\lambda_{PM,a}}{dt} + \frac{d\lambda_{PM,b}}{dt}\right). \end{aligned} \tag{10}$$

Under fault condition, the symmetry of the PMSM is destroyed. Based on the principle of the identical equation, it is seen from (10) that, besides the $3n(n = 1, 3, 5, \ldots)$ order harmonic components, the fundamental component and other harmonic components are present in the i_{zsc}, compared with the healthy condition. Furthermore, the amplitude of the fundamental component is the largest among those of the new added harmonic component. Consequently, the open-phase fault in the delta-connected PMSM can be detected by the fundamental component of the i_{zsc}.

Since only the fundamental component of the ZSCC i_{zsc} is considered, (10) can be simply written as

$$R_s i_{zsc} + (L + M)\frac{di_{zsc}}{dt} = N\sin(\theta + \theta_f) \tag{11}$$

where N and θ_f are the amplitude and initial phase angle of the fundamental component, respectively.

In (11), if θ is regarded as an independent variable and i_{zsc} is regarded as a dependent variable. Thus, (11) is a first-order nonhomogeneous linear differential equation with constant coefficients. Hence, i_{zsc} can be calculated as

$$\begin{aligned} i_{zsc} &= \frac{N}{\sqrt{(\omega_e(L + M))^2 + {R_s}^2}}\sin(\theta + \theta_f + \gamma) \\ &= I_1\sin(\theta + \beta) \end{aligned} \tag{12}$$

TABLE I
AUXILIARY FAULT INDICATOR

State	a_a	a_b	a_c
Healthy	1	1	1
Fault in phase *a*	0	2	2
Fault in phase *b*	2	0	2
Fault in phase *c*	2	2	0

TABLE II
SPECIFIC PARAMETERS OF PMSM

PMSM	Value	PMSM	Value
Rated Power (W)	550	Rated Speed (r/min)	1500
Rated Torque (N.m)	3.5	Self-inductance (H)	0.13
Number of Pole Pairs	2	Mutual-inductance (H)	–0.03
Stator Resistance (Ω)	10.5	Permanent Magnet Flux Linkage (Wb)	0.636

where ω_e is the electrical angle speed of the PMSM, I_1 and ˜β are expressed as

$$I_1 = \frac{N}{\sqrt{(\omega_e(L+M))^2 + R_s^2}} \qquad \beta = \theta_f + \gamma \tag{13}$$

where γ is a variable and is expressed as

$$\gamma = \tan^{-1}(-\omega_e(L+2M)/R_s). \tag{14}$$

C. Fault Indicator

To achieve fault detection, neglecting the variations of the PMSM parameters (R_s, L, and M), the fault indicator is defined as

$$\mathrm{FI} = I_1\sqrt{R_s^2 + \omega_e^2(L+M)^2}/U_{dc} = N/U_{dc} \tag{15}$$

where FI is the fault indicator and U_{dc} is the dc-link voltage. Based on the previous analysis, the fault indicator FI is nearly close to zero under healthy condition since the fundamental component of the i_{zsc} does not exist.

For the delta-connected PMSM, the stator current of the faulty phase is equal to zero. To locate the faulty phase without the influence of the PMSM load, the auxiliary fault indicator is defined as

$$a_n = \frac{2\langle|i_n|\rangle}{\langle|i_l|\rangle + \langle|i_m|\rangle} \tag{16}$$

where $l, m, n \in \{a, b, c\}$ and $l \neq m \neq n$. $\langle|i_j|\rangle$ $(j = l,\ m,\ n)$ denotes the mean value of the absolute value of i_j, and the calculation process is expressed as

$$\langle|i_j|\rangle = \frac{\omega_e}{2\pi}\int_0^{\frac{2\pi}{\omega_e}} |i_j|dt. \tag{17}$$

Theoretically, a_j is equal to zero under healthy condition. As the fault occurs in the phase n, a_n is equal to zero, a_l and a_m are both equal to two. As the fault occurs in other phases, the similar results can be obtained by analogy. The detailed results are listed in Table I.

D. Fault Detection and Location

To obtain the fault indicator, the amplitude of the fundamental component of the ZSCC is required to be tracked. In this letter, a simple and effective frequency tracking algorithm is adopted, the detailed description can be addressed to [18]. The auxiliary fault indicators can be calculated online.

After the amplitude of the fundamental component of the ZSCC calculated by frequency tracking algorithm, and then the fault indicator can be obtained based on (15). If the fault indicator is larger than the preset threshold, which is corresponding to its value for the healthy PMSM, the fault is detected. Once the fault is detected, the faulty phases are identified based on the auxiliary fault indicator in Table I.

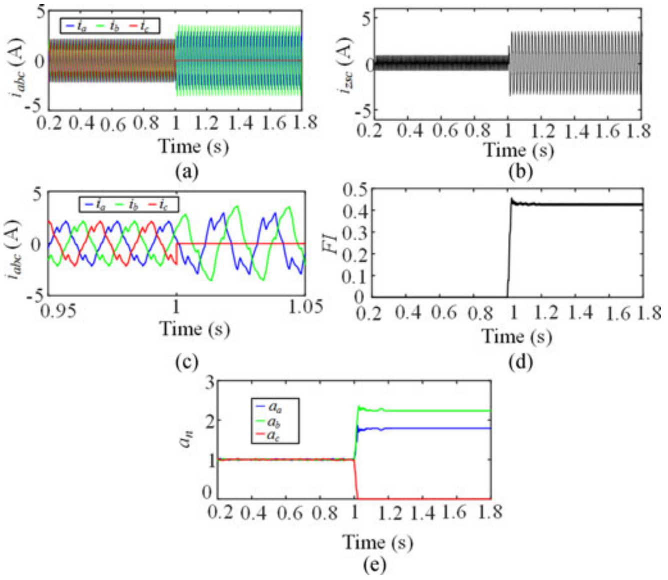

Fig. 2. Simulation results of the fault in phase c, at a reference speed 480 r/min with 50% rated load. (a) Stator current. (b) ZSCC. (c) Stator current. (d) Fault indicator. (e) Auxiliary fault indicator.

In addition, this work can detect the open-phase fault and identify the faulty phase, which can make the maintenance personnel achieve the targeted maintenance or can prepare for adapting the fault-tolerant control strategy. Hence, the reliability of the PMSM is greatly improved, thus, improving the reliability of the industry.

IV. SIMULATION AND EXPERIMENTAL VALIDATION

A. Simulation Validation

To validate the effectiveness of the proposed method, the simulation is carried out in the MATLAB/Simulink environment. In the simulation, the PMSM is controlled by the $i_d = 0$ control strategy employing current hysteresis. Table II lists the specific parameters of the studied PMSM.

Fig. 2 shows the simulation results of the stator currents, ZSCC, fault indicator, and auxiliary fault indicator, where the delta-PMSM operates at a reference speed 1500 r/min with the rated load. It is seen that the fault indicator is equal to zero and three auxiliary fault indicators are all equal to one under healthy

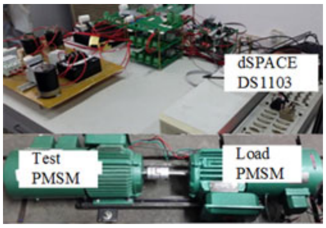

Fig. 3. Experimental platform.

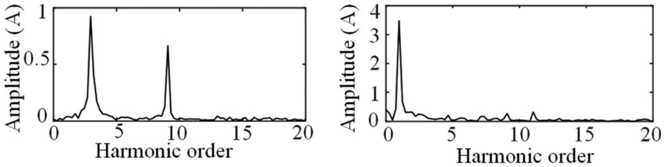

(a) (b)

Fig. 4. FFT results of ZSCC i_{zsc} under healthy and open-phase fault condition. (a) Healthy. (b) Open-phase fault in phase c.

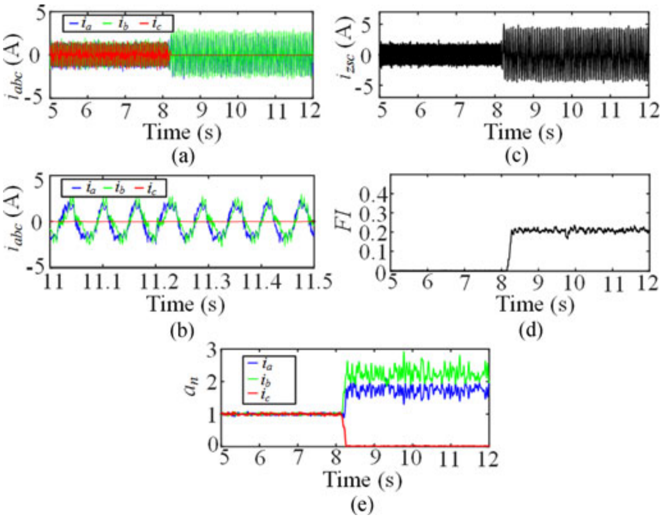

Fig. 5. Experimental results of the fault in phase c, at a reference speed 480 r/min with 50% rated load. (a) Stator current. (b) Stator current. (c) ZSCC. (d) Fault indicator. (e) Auxiliary fault indicator.

condition. At the instant $t = 1$ s, the open-phase fault occurs in the phase c. It can be seen that the stator current i_c is changed into zero and the amplitudes of the stator currents i_a and i_b increase. The fault indicator quickly increases and converges to 0.43, and three auxiliary fault indicators a_a, a_b, and a_c are changed and converges to 1.8, 2.3, and 0, respectively. Hence, the open-phase fault can be detected through the difference of the fault indicator between nonfault and fault states. There is a certain difference between the simulation results and the theoretical value for the auxiliary fault indicators. However, the auxiliary fault indicators can be still used to identify the faulty phase.

B. Experimental Validation

The experimental platform is set up to further validate the proposed method, as shown in Fig. 3, mainly including two PMSMs. Two PMSMs are directly connected through one coupling, where one is used as test machine, and the other one is used as load machine. The dSPACE is used to control the PMSMs. The test PMSM is controlled by the $i_d = 0$ control strategy employing current hysteresis. The load torque of the test PMSM is imposed by a load PMSM controlled by the $i_d = 0$ method. The parameters of two PMSMs are the same, just the stator winding connection mode is different. The connection modes of the test and load PMSMs are delta-connected and wye-connected, respectively. The parameters of two PMSMs are the same as those listed in Table II.

It should be noted that, as the open-phase fault occurs in the PMSM, the high speed or overload may lead to the damage to the PMSM or the whole system, so the experiments are performed at low speed and low load to avoid secondary failure. To evaluate the diagnostic effectiveness, four different operation statuses, namely 50% rated load at a reference speed 360 r/min, 25% rated load at a reference speed 360 r/min, 50% rated load at a reference speed 480 r/min, and 25% rated load at a reference speed 480 r/min are studied.

Fig. 4 shows the fast Fourier transform (FFT) results of the ZSCC i_{zsc} under healthy and open-phase fault condition, where the PMSM operate at a reference speed 480 r/min with 50% rated load. It can be seen that the ZSCC i_{zsc} is constituted by the third harmonic component and ninth harmonic components under healthy condition. In the case of the open-phase fault, the fundamental component appears in the ZSCC i_{zsc}. Hence, it is shown that the experimental results agree with the theoretical analysis.

Fig. 5 shows the experimental results of the stator currents, ZSCC, fault indicator, and auxiliary fault indicator, where the delta-PMSM operates at a reference speed 480 r/min with 50% rated load. It can be seen that the fault indicator is close to zero and three auxiliary fault indicators are all nearly equal to one. At the instant $t = 8.22$ s, the open-phase fault occurs in the phase c. It is seen that the stator current i_c is changed into zero. The amplitudes of the stator currents i_a and i_b increase, and the waveforms of the stator currents i_a and i_b are nearly same with a certain phase difference. The fault indicator increases and converges to 0.2, and three auxiliary fault indicators a_a, a_b, and a_c are changed into 1.7, 2.3, and 0, respectively. Hence, the open-phase fault can be detected through the variation of the fault indicator. There is a certain difference in the auxiliary fault indicators, compared with the theoretical value. However, the faulty phases can be still identified by the auxiliary fault indicators.

To further validate the effectiveness of the proposed method, the experiments are performed at three different operating points, where the open-phase fault occurs in the phase c of the test PMSM. The experimental results are presented in Figs. 6–8. It can be seen that, under healthy condition, the fault indictor is close to zero and the auxiliary fault indicators are nearly equal to one. Under open-phase fault condition, the fault is affected by the operating point. However, the open-phase fault can be still detected through the difference of the fault indicator between healthy and fault states. It can be also seen that, under open-phase fault condition, the variation of the operating point has a certain influence on three auxiliary fault indicators. However, the faulty phases can be still identified by the auxiliary fault indicators.

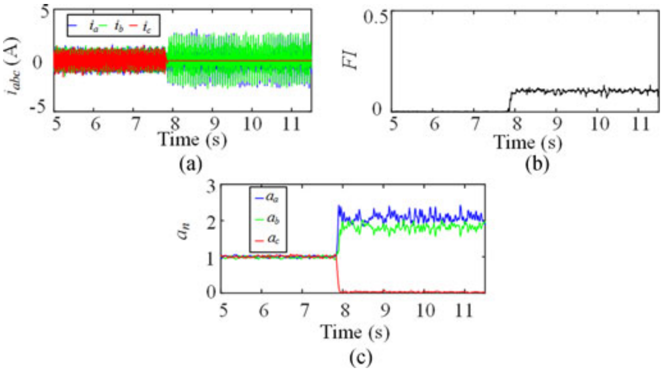

Fig. 6. Experimental results of the fault in phase c, at a reference speed 480 r/min with 25% rated load. (a) Stator current. (b) Fault indicator. (c) Auxiliary fault indicator.

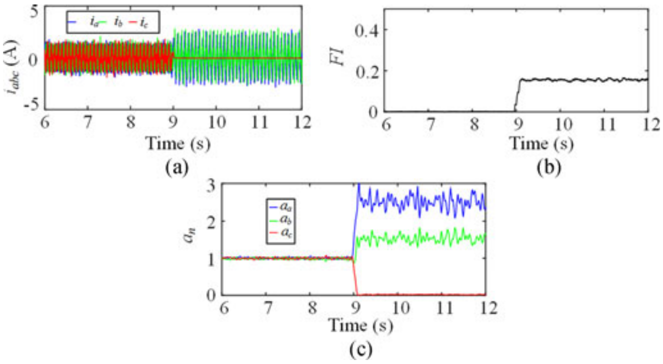

Fig. 7. Experimental results of the fault in phase c, at a reference speed 360 r/min with 50% rated load. (a) Stator current. (b) Fault indicator. (c) Auxiliary fault indicator.

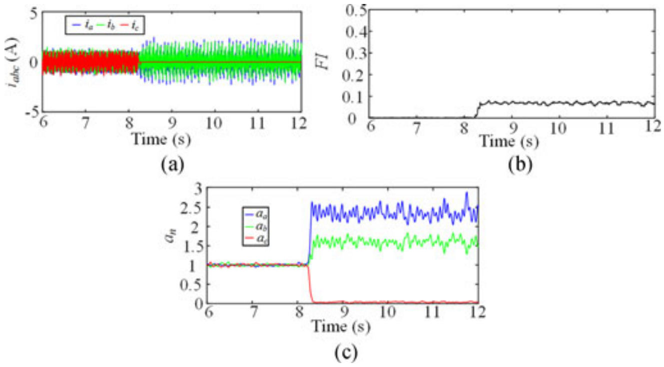

Fig. 8. Experimental results of the fault in phase c, at a reference speed 360 r/min with 25% rated load. (a) Stator current. (b) Fault indicator. (c) Auxiliary fault indicator.

V. CONCLUSION

In this letter, the open-phase fault detection method is proposed for the delta-connected PMSM drive systems, which is based on ZSCC and stator currents. The open-phase fault can be detected by the fault indicator, and the faulty phase can be located by the auxiliary fault indicator. Both the simulation and experimental results confirm the validity of the proposed method.

REFERENCES

[1] M. Cheng, J. Hang, and J. Zhang, “Overview of fault diagnosis theory and method for permanent magnet machine,” *Chin. J. Elect. Eng.*, vol. 1, no. 1, pp. 21–36, Dec. 2015.

[2] B. A. Welchko, T. A. Lipo, T. M. Jahn, and S. E. Schulz, “Fault tolerant three-phase AC motor drive topologies: A comparison of features, cost, and limitations,” *IEEE Trans. Power Electron.*, vol. 19 no. 4, pp. 1108–1116, Jul. 2004.

[3] D. U. Campos-Delgado, D. R. Espinoza-Trejo, and E. Palacios, “Fault tolerant control in variable speed drives: A survey,” *IET Elect. Power Appl.*, vol. 2, no. 2, pp. 121–134, Mar. 2008.

[4] W. Wang, J. Zhang, and M. Cheng, “Common model predictive control for permanent-magnet synchronous machine drives considering single-phase open-circuit fault,” *IEEE Trans. Power Electron.*, vol. 32, no. 7, pp. 5862–5872, Oct. 2016.

[5] A. Kontarcek, P. Bajec, M. Nemec, V. Ambrozic, and D. Nedeljkovic, “Cost-effective three-phase PMSM drive tolerant to open-phase fault,” *IEEE Trans. Ind. Electron.*, vol. 62, no. 11, pp. 6708–6718, May 2015.

[6] A. Gaeta, G. Scelba, and A. Consoli, “Modeling and control of three-phase PMSMs under open-phase fault,” *IEEE Trans. Ind. Appl.*, vol. 49, no. 1, pp. 74–83, Jan./Feb. 2013.

[7] F. Lin, Y. Hung, and M. Tsai, “Fault-tolerant control for six-phase PMSM drive system via intelligent complementary sliding-mode control using TSKFNN-AMF,” *IEEE Trans. Ind. Electron.*, vol. 60, no. 12, pp. 5747–5762, Dec. 2013.

[8] H. Dang, Z. Zhu, and M. Foster, “Direct torque control of permanent magnet brushless AC drive with single-phase open-circuit fault accounting for influence of inverter voltage drop,” *IET Elect. Power Appl.*, vol. 7, no. 5, pp. 369–380, May 2013.

[9] G. Catuogno, G. Garcia, and R. Leidhold, “Fault tolerant control in six-phase PMSM under four open-circuits fault conditions,” in *Proc. 42nd Annu. Conf. IEEE Ind. Electron. Soc.*, 2016, pp. 5754–5759.

[10] S. Ahmed and N. Demerdash, “Fault-tolerant operation of delta-connected scalar-and vector-controlled AC motor drives,” *IEEE Trans. Power Electron.*, vol. 27, no. 6, pp. 3041–3049, Jun. 2012.

[11] A. Gaeta, G. Scelba, and A. Consoli, “Sensorless vector control of PM synchronous motors during single-phase open-circuit faulted conditions,” *IEEE Trans. Ind. Appl.*, vol. 48, no. 6, pp. 1968–1979, Nov./Dec. 2012.

[12] C. J. Gajanayake, B. Bhangu, S. Nadarajan, and G. Jayasinghe, “Fault tolerant control method to improve the torque and speed response in PMSM drive with winding faults,” in *Proc. IEEE 9th Int. Conf. Power Electron. Drive Syst.*, 2011, pp. 956–961.

[13] A. Khlaief, M. Boussak, and M. Gossa, “Open phase faults detection in PMSM drives based on current signature analysis,” in *Proc. IEEE XIX Int. Conf. Elect. Mach.*, 2010, pp. 1–6.

[14] A. Kontarcek, P. Bajec, M. Nemec, and V. Ambrozic, “Single open-phase fault detection in permanent magnet synchronous machine through current predication,” in *Proc. 39th Annu. Conf. IEEE Ind. Electron. Soc.*, 2013, pp. 5860–5865.

[15] S. S. Kuruppu and A. Kulatunga, “D-Q current signature based faulted phase localization for SM-PMAC machine drive,” *IEEE Trans. Ind. Electron.*, vol. 2, no. 1, pp. 113–121, Jan. 2015.

[16] J. Hang, J. Zhang, M. Cheng, and S. Ding, “Detection and discrimination of open-phase fault in permanent magnet synchronous motor drive system,” *IEEE Trans. Power Electron.*, vol. 31, no. 7, pp. 4697–4709, Jul. 2016.

[17] A. Arafat, S. Choi, and J. Baek, “Open phase fault detection of a five-phase permanent magnet assisted synchronous reluctance motor based on symmetrical components theory,” *IEEE Trans. Ind. Electron.*, vol. 64, no. 8, pp. 6465–6474, Aug. 2017.

[18] J. Hang, J. Zhang, M. Cheng, and J. Huang, “Online interturn fault diagnosis of permanent magnet synchronous machine using zero-sequence components,” *IEEE Trans. Power Electron.*, vol. 30, no. 12, pp. 6731–6741, Dec. 2015.